Compact 300-J/300-GW Frequency-Doubled Neodymium Glass Laser—Part I: Limiting Power by Self-Focusing

Anatoly K. Potemkin, Efim A. Khazanov, Mikhail A. Martyanov, and Mar'yana S. Kochetkova

***Abstract*—Small-scale self-focusing is the main cause of power limitation in nanosecond Nd:glass lasers. We report pioneer observation in experiment of laser beam noise amplification for B-integral (nonlinear phase) order of unity, i.e., without destruction of nonlinear medium. Analytical dependences of noise amplification coefficient on the B-integral have been obtained for one nonlinear medium as well as for two nonlinear media separated by an air gap with image relay. A simple analytical dependence has been found for an optimal distance between two nonlinear media for which the maximum allowable value of B-integral increases from 2.7 to 4.3. The maximum attainable energy in neodymium-phosphate glass lasers with rod amplifiers 10 cm in diameter is 400 J with a pulse duration of 1 ns.**

***Index Terms*—B-integral, Nd:glass laser, nonlinear refractive index, self-focusing.**

I. Introduction

RECENT investigations demonstrated that the use of the chirped pulse amplification technique in super-broadband parametric amplifiers makes it possible to create compact femtosecond laser systems with petawatt power [1]. The last cascade of the parametric amplifier in such systems is pumped by the second harmonic of a neodymium-phosphate glass pulsed laser. This laser is one of the most expensive and large-size parts of the system. To attain the petawatt level, the energy of 150–200 J at the second harmonic in a pulse with a duration of 1 ns is needed, which demands not less than 300 J at the fundamental harmonic.

Lasers having such parameters described in the literature [2] occupy vast areas and are difficult to maintain. This is explained by the use of inefficient laser amplifiers and extremely complicated schemes, when optical isolators based on Faraday rotators or Pockels cells are installed after each amplification cascade. The goal of the current work is to create a relatively inexpensive, compact (table-top) laser that would be simple, reliable, and easy to operate.

Active elements of a laser are, primarily, of two shapes: rods and disks. Disk amplifiers are, as a rule, more complicated for fabrication and operation; therefore, disks are employed only when rods cannot be used. The diameter of rod amplifiers is limited by a possibility of pumping the central area (maximal diameter is $10 \div 15$ cm), and their length by inversion reduction due to amplified spontaneous emission (ASE) (maximal length is 20–30 cm) [3].

The basic cause of power limitation in pulsed lasers is the destruction of optical elements by breakdown and self-focusing [2], [4], [5]. The damage threshold is usually estimated to be about $w_{\rm th} = 10$ J/cm^2 for a laser pulse duration of 1 ns [6]. The energy limited by damage threshold is $W_{\rm th} = w_{\rm th} F \pi D^2/4$, where D is the active element diameter and F is the fill-factor. Hereinafter, we assume the beam to be axially symmetric. For $D = 10$ cm and $F = 0.8$, we obtain $W_{\rm th} = 600$ J. Thus, development of a 300-J/300-GW laser with output rod amplifier 10 cm in diameter is not restricted by damage threshold.

The change of the beam spatial structure stipulated by the dependence of the refractive index n on light intensity I

$$n = n_0 + n_2 |E|^2/2 = n_0 + \gamma I \tag{1}$$

where n_0 is the linear refractive index and

$$\gamma = 4\pi n_2/(cn_0)[\text{esu}] \approx 4.19 \cdot 10^{-3} n_2/n_0\,[\text{cm}^2/\text{W}]$$

characterizes cubic nonlinearity of a dielectric is called self-focusing or self-action [7]. Typical values for nanosecond pulses are $n_2 = (1 \div 3) \cdot 10^{-13}$ esu and $\gamma = (3 \div 8) \cdot 10^{-7}$ cm^2/GW [7], [8]. Consequently, optical beams with an intensity close to the damage threshold intensity of a transparent dielectric of 10 GW/cm^2 change the refractive index by about $(3 \div 8) \cdot 10^{-6}$. However, for a long nonlinear medium, even such small changes in n may result in catastrophic deterioration of beam quality and in destruction of the medium.

Two limiting cases of self-focusing may be distinguished. These are large-scale self-focusing (LSSF), which will be addressed in Section II, and small-scale self-focusing (SSSF), which will be considered in detail analytically, numerically, and experimentally in Section III. In particular, experimental observation of SSSF at small radiation power will be described.

II. Large-Scale Self-Focusing

LSFF, i.e., self-focusing of a beam as a whole, is especially pronounced in beams with a strong radial dependence of intensity. As is clear from (1), the refractive index repeats the intensity profile; hence, the peripheral rays of the beam refract to its axis, thus causing beam focusing. The beam power at which diffraction is compensated completely by such nonlinear refraction is referred to as critical self-focusing power $P_{\rm cr}$. For a Gaussian-profile beam, $P_{\rm cr} = 35.3\lambda^2/n_2 = 0.174\lambda^2/(\gamma n_0)$

Manuscript received July 31, 2008; revised October 28, 2008. Current version published March 11, 2009.

The authors are with the Institute of Applied Physics, Russian Academy of Science, Nizhny Nvogorod 603000, Russia.

Digital Object Identifier 10.1109/JQE.2009.2013212

[9], where λ is the wavelength in vacuum. A typical value of $P_{\rm cr}$ is $(1 \div 4)$ MW.

The medium length on which self-focusing of a Gaussian beam having radius a leads to its collapse was found numerically in [9] to be

$$L_{\rm LS} = \frac{2.3a^2}{\lambda\sqrt{(\sqrt{P/P_{\rm cr}} - 0.825)^2 - 0.03}}. \tag{2}$$

In laser amplifiers, the medium length L is, as a rule, much less than $L_{\rm LS}$. In this case, the nonlinear medium only distorts the wave front. If the beam at the input to the nonlinear medium has a plane wave front, then at the output its phase will be

$$\Psi(r) = B(r) = \frac{2\pi}{\lambda}\gamma\int_0^L I(r,z)dz \tag{3}$$

which is called the breakup integral or B-integral. The increase of the angular spread of the beam caused by the phase equation (3) may be partially compensated by a lens with focal length $F_{\rm corr}$. In accordance with the ISO 11146 standard, we will take parameter M^2 as a criterion of least beam divergence [10]. By calculating moments of beam intensity for an arbitrary profile beam [11], we can find the value of $F_{\rm corr}$ ensuring minimal M^2. For a beam with super-Gaussian intensity distribution $I(r) = I_0\exp((r/a)^{2N})$, we found [12], [13] divergence before correction ϑ, $F_{\rm corr}$, and residual divergence after correction $\vartheta_{\rm corr}$ as

$$\begin{aligned}
\vartheta &= \frac{\lambda}{2\pi a}\sqrt{\frac{N^2}{\Gamma(1/N)} + \left(1 + \frac{4}{9}B^B\right)} \\
F_{\rm corr} &= \frac{2\pi a^2}{\lambda B}2^{-1/N}\frac{\Gamma(2/N)}{\Gamma(1/N)} \\
\vartheta_{\rm corr} &= \frac{\lambda}{2\pi a}\sqrt{\frac{N^2}{\Gamma(1/N)} + \left(\frac{4N^N}{9\Gamma(1/N)} - 2^{-2/N}\frac{\Gamma(1/N)}{\Gamma(2/N)}\right)B^2}
\end{aligned} \tag{4}$$

where Γ is the Euler gamma function.

If the nonlinear medium is amplifying, then the value of the nonlinear length $L_{\rm LS}$ will differ from (2). However, the condition $L \ll L_{\rm LS}$ will be fulfilled, as a rule, and the expressions in (4) remain valid. Thus, radiation output power enhancement caused by additional amplifiers is inevitably accompanied by increasing beam divergence due to LSSF, which reduces beam brightness. An expression for the limiting value of the B-integral in terms of maximal radiation brightness was presented in [14].

Note that, similarly to intensity, the B-integral is time-dependent. Consequently, divergence due to the LSSF equation (4) also changes within the pulse. Expressions for the maximal value of the B-integral and for the corresponding moment of time with allowance for laser amplification were found in [15].

III. Small-Scale Self-Focusing

As was shown in the previous section, LSSF in powerful laser systems does not lead to catastrophic beam collapse; it only increases its divergence. At the same time, Bespalov and Talanov in their work [4] showed that, in a cubic nonlinear medium, small-scale amplitude or phase spatial inhomogeneities that are always present in the beam may be amplified in the presence of a powerful wave. This results in disintegration of the beam into separate filaments, i.e., in SSSF. Below, we will consider some SSSF aspects that are principal for laser amplifiers: transformation matrix of perturbations, angular spectrum of amplified noise, noise amplification coefficient integral over the spectrum, allowance for the air gap between successively located nonlinear media, and the influence of laser amplification.

A. Transformation Matrix of Perturbations

Each harmonic perturbation with spatial frequency (transverse wave vector) $k_\perp$ may be correlated to a pair of plane waves propagating at angles $\alpha = \pm k_\perp/k$ to an intense wave, where $k = 2\pi n_0/\lambda$. In what will follow, we will use the normalized spatial frequency

$$\kappa = k_\perp\sqrt{L/k}. \tag{5}$$

Weak perturbation of an arbitrary shape may be represented as a sum of plane waves. By calculating the increment of each individual wave and changes of its phase, one can find the shape of the perturbation at the nonlinear medium output. Bespalov and Talanov [4] showed within the framework of the linearized theory that perturbations are unstable in the spatial frequency band

$$0 < \kappa < \kappa_{\rm cr} = 2\sqrt{B} \tag{6}$$

where frequency $\kappa_{\max}$ at which amplification is maximal is defined by

$$\kappa_{\max} = \sqrt{2B}. \tag{7}$$

At large values of B-integral, the beam disintegrates into separate filaments, each of which contains the power of order $P_{\rm cr}$ [4]. Filaments collapse on the characteristic length $L_{\rm SS} \approx ka^2P_{\rm cr}/P$, which is inevitably accompanied by breakdown. From (2), one can readily show that $L_{\rm SS}/L_{\rm LS} \approx \sqrt{P_{\rm cr}/P}$. Consequently, if $P \gg P_{\rm cr}$, then $L_{\rm SS} \ll L_{\rm LS}$, i.e., SSSF is always the main cause of power limitation in powerful laser systems.

Let us write complex amplitude of perturbation $\boldsymbol{\varepsilon}$ in the form of a real vector

$$\boldsymbol{\varepsilon} = \begin{pmatrix} {\rm Re}\varepsilon \\ {\rm Im}\varepsilon \end{pmatrix} = |\boldsymbol{\varepsilon}| \cdot \begin{pmatrix} \cos\varphi \\ \sin\varphi \end{pmatrix} \tag{8}$$

where φ is the phase difference between the perturbation and the powerful wave. Complex amplitudes of perturbation at the input $\boldsymbol{\varepsilon}_{\rm in}$ and at the output $\varepsilon_{\rm out}$ of the nonlinear medium are related by transformation matrix $\mathbf{U}$

$$\boldsymbol{\varepsilon}_{\rm out} = \mathbf{U}\boldsymbol{\varepsilon}_{\rm in}. \tag{9}$$

As was shown in [5], the transformation matrix has the form

$$\mathbf{U} = \begin{pmatrix} \cosh(Bx) & -\frac{\kappa^2}{2Bx}\sinh(Bx) \\ \frac{\kappa^2 - 4B}{2Bx}\sinh(Bx) & \cosh(Bx) \end{pmatrix} \tag{10}$$

where $x^2 = \kappa^2/B - \kappa^4/(4B^2)$, i.e., all of the elements of matrix $\mathbf{U}$ are functions of spatial frequency κ and the B-integral only. Knowing the phase delay between the powerful wave and the

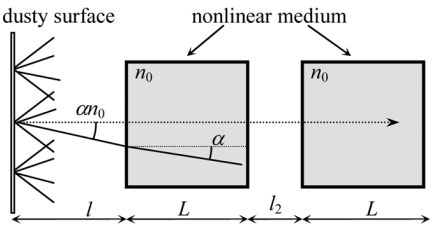

Fig. 1. Geometry of the problem. Kepler telescope placed behind a dusty surface as well as between nonlinear media gives $l < 0$ and $l_2 < 0$.

perturbation at the input to the nonlinear medium $\varphi_{\rm in}$ from (9) and (10), one can easily calculate amplification coefficient of intensity perturbation $K = |\varepsilon_{\rm out}|^2/|\varepsilon_{\rm in}|^2$ and phase delay at the output $\varphi_{\rm out}$ as

$$K = \left(u_{12}^2 + u_{22}^2\right)\sin^2\varphi_{\rm in} + \ldots + \left(u_{11}^2 + u_{21}^2\right)\cos^2\varphi_{\rm in} + \ldots + \left(u_{11}u_{12} + u_{21}u_{22}\right)\sin 2\varphi_{\rm in} \quad (11)$$

$$\varphi_{\rm out} = \arctan\left(\frac{u_{21} + u_{22}\tan\varphi_{\rm in}}{u_{11} + u_{12}\tan\varphi_{\rm in}}\right). \quad (12)$$

It is apparent from (10)–(12) that K and $\varphi_{\rm out}$ depend on the spatial frequency of the perturbation κ, B-integral, and input phase of the perturbation $\varphi_{\rm in}$.

B. Angular Spectrum of Noise Amplified at SSSF

For further analysis, let us specify the noise source. Consider the perturbation arising when the beam passes through a dusty surface (Fig. 1). It may be represented as a superposition of plane waves, with all of the waves in the plane of the surface be in-phase with the powerful wave: $\varphi = 0$. When the waves are propagating along the z axis in free space, their phases shift and at the input to the nonlinear medium located at distance l from the dusty surface the input phase of the perturbation will be

$$\varphi_{\rm in} = \frac{\alpha^2}{2} k n_0 l \quad (13)$$

where $\alpha = k_\perp/k = \kappa/\sqrt{kL}$ is the angle at which the perturbation wave propagates in the nonlinear medium.

The function $K(\varphi_{\rm in}, \alpha/\alpha_{\max})$, where $\alpha_{\max} = \kappa_{\max}/\sqrt{kL}$, is plotted in Fig. 2. The picture will be mirror symmetric for negative angles α. The function $K(\varphi_{\rm in})$ is a sinusoid for arbitrary α. For $\alpha = \alpha_{\max}$, this sinusoid has maximal amplitude: $K_{\max} = \exp(2B)$ and $K_{\min} = \exp(-2B)$. When $\alpha \to 0$, then, from (10) and (13), we obtain $K(\alpha = 0) = 1 + 4B^2$. Spatial filters do not attenuate noise at small α; therefore, in a multicascade amplifier, K may attain rather high values at low spatial frequencies.

From (11), it follows that, on the $(\varphi_{\rm in}, \alpha)$ plane, one can draw the curves [16]

$$\varphi_{\rm in}^{\max} = -\frac{\pi}{4} - \frac{1}{2}\arctan\left(\frac{\kappa^2 - 2B}{2Bx}\tanh(Bx)\right) + \pi m \quad (14)$$

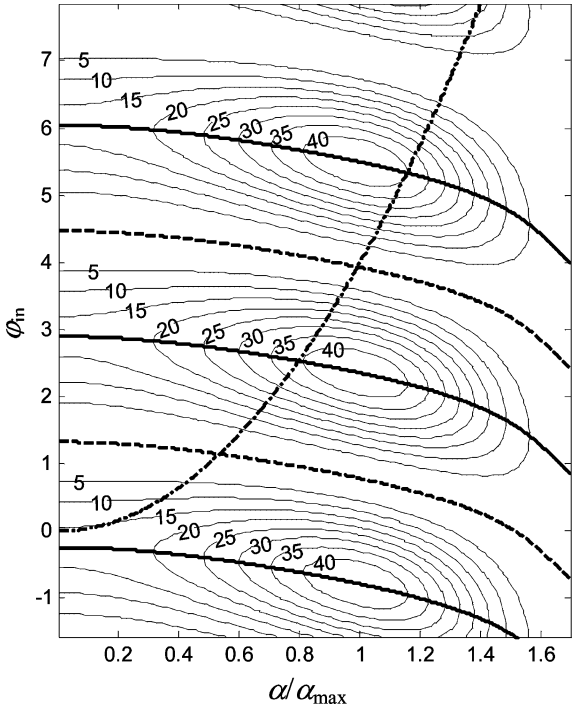

Fig. 2. Lines of the same level for the function $K(\varphi_{\rm in}, \alpha/\alpha_{\max})$ at $B = 1.9$. Solid and dotted lines are for the curves (14) and (15), and the dot–dashed line is for the parabola (13) at $l = 100$ cm.

on which K has maximal value and the curves

$$\varphi_{\rm in}^{\min} = -\frac{\pi}{2} + \varphi_{\rm in}^{\max} \quad (15)$$

on which K is minimal (here m are integers). These curves are plotted in Fig. 2 by heavy solid and dotted lines.

The function $\varphi_{\rm out}(\varphi_{\rm in}, \alpha/\alpha_{\max})$ is plotted in Fig. 3. It is clear from the figure that $\varphi_{\rm out}$ weakly depends on $\varphi_{\rm in}$, i.e., in the case of noise from a dusty surface located at distance l from a nonlinear medium, the output perturbation phase $\varphi_{\rm out}$ weakly depends on l. This allows one to suppress SSSF in two nonlinear media (see Section III-D).

Figs. 2 and 3 and the expressions (11)–(12) are handy for analysis of the spatial noise spectrum at SSSF. For example, if total noise power $P_{\rm n}$ is caused by diffraction of a beam of diameter D on dust particles having diameter $d \ll D$ that are located on the surface at distance l from the nonlinear medium, then the picture of SSSF will be the following. Perturbation within angle $2\alpha_{\rm dust} = 2.44\ \lambda/d$ will propagate from each dust particle. Perturbations from individual dust particles will interfere at the input to the nonlinear medium and the intensity distribution will be randomly modulated. A bright spike in the angle $2.44\lambda/D$ will occur in the far field, as well as noise speckled with the same scale and spread in the angle $2\alpha_{\rm dust}$. Different angular components at the input to the nonlinear medium have different phases depending on l in accord with the parabolic dependence (13) plotted in Fig. 2 for $l = 100$ cm. One can see in the figure that, as angle α increases, K successively takes on minimal (for $\alpha = 0.55\ \alpha_{\max}, 0.98\alpha_{\max}$) and maximal (for $\alpha = 0.8\alpha_{\max}, 1.15\alpha_{\max}$) values. Thus, noisy radiation that has passed through a nonlinear medium will have a ring structure in

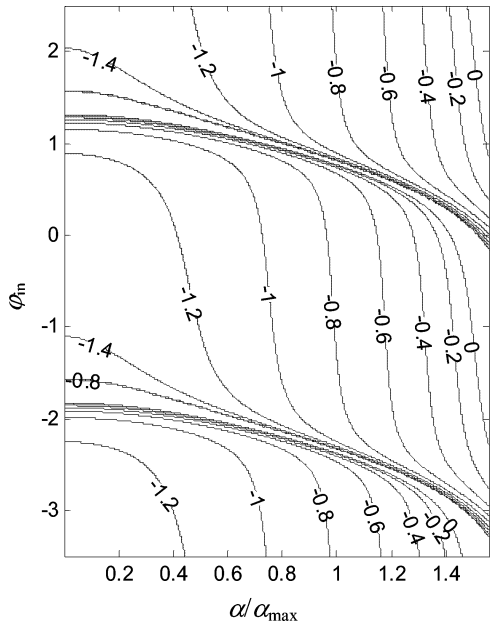

Fig. 3. Lines of the same level for the function $\varphi_{\rm out}(\varphi_{\rm in}, \alpha/\alpha_{\rm max})$ at $B = 1.9$.

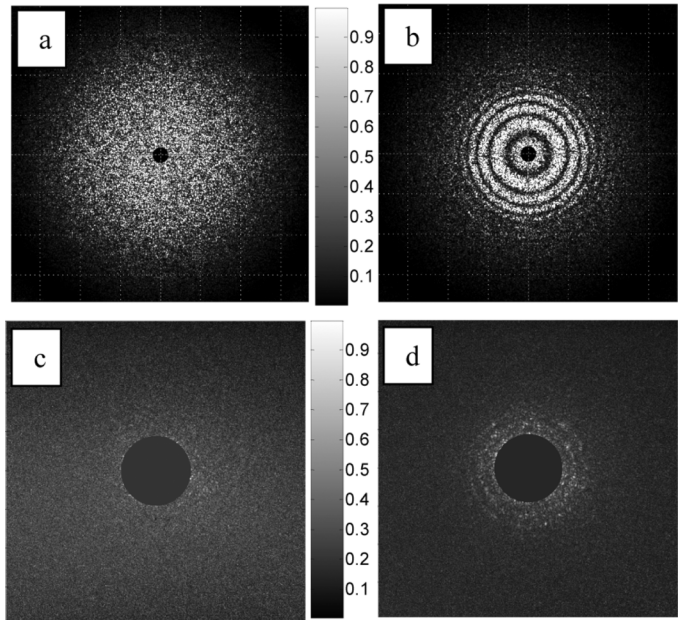

Fig. 4. (a), (b) Numerical and (c), (d) measured distributions of noise component in the far field for (a), (c) $B = 0$ and (b), (d) $B = 1.15$.

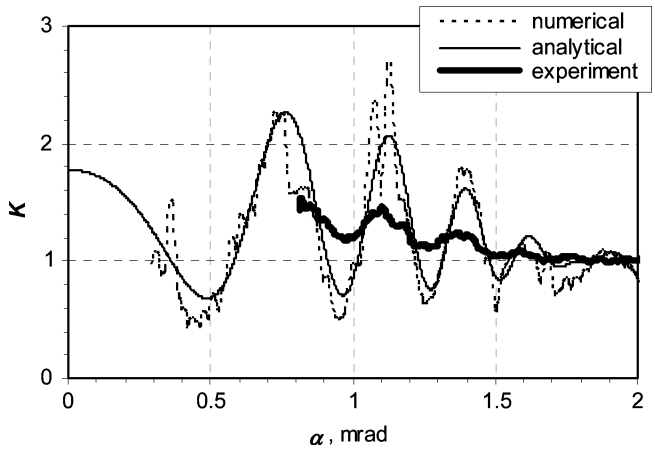

Fig. 5. Analytical (11), numerical, and experimental function $\mathrm{K}(\alpha)$ for $B = 1.15, l = 135$ cm.

the far field. Note that K will not necessarily take on the maximal value at $\alpha = \alpha_{\max}$, and it may be more than unity outside the instability band (6).

Analogous parabolas (13) may be plotted for other values of l, including its negative values that may be readily achieved by relaying the images of dusty surface by means of a Kepler telescope.

Let us illustrate the above considerations by numerical simulation of SSSF using the FRESNEL software [16]. A flat-top beam (diameter D $= 4$ cm, $\lambda = 1$ μm, power $P = 10$ GW) propagated through a screen with dust particles having diameter $d = 0.02$ cm. Losses due to the dust particles were 2.5%, i.e., the total noise power was $P_{\rm n} = 0.25$ GW. Beam divergence of the main beam was $2.44\lambda/D = 61$ μrad, and beam divergence of the noise component was 2.44 $\lambda/d = 12.2$ mrad. At distance $l = 135$ cm from the screen, there was a nonlinear medium 63 cm long with $n_0 = 1.534$ and $n_2 = 1.2 \cdot 10^{-13}$ esu, which corresponds to $B = 1.15$ for $I = 1$ GW/cm^2. Numerical computation was done by a rectangular grid 2048×2048. The main beam was screened in the far field so as not to interfere with noise component distribution. The far field of noise for $B = 1.15$ is depicted in Fig. 4(a) and (b). It has a ring structure in full correspondence with the analytical results presented above (Fig. 5).

For verification of the above analytical and numerical results, the following experiment was performed. A laser beam reflected from a dielectric mirror with defects having diameter $d = 100 \div 200$ μm randomly scattered over the surface. Losses induced by these defects were 2.4%. The beam passed through a 63-cm-long rod of silica-based neodymium glass ($n_0 = 1.534$ and $n_2 = 1.2 \cdot 10^{-13}$ esu [8]) and was focused by a lens with a focal distance 73 cm. For the radiation of the main beam not to affect the CCD camera, a mirror with a hole 0.65 mm in diameter was placed in the focal plane. As a result, a powerful wave passed through the hole and the noise component on reflection at this mirror was projected by image relay to the CCD camera.

Results of the measurements are presented in Fig. 4(c) and (d). For the linear case ($B = 0$), the angular distribution of noise is uniform, whereas for $B \approx 1$ rings appear in the noise distribution. The bright rings correspond to transverse scales with maximal amplification, and the dark rings to the scales on which the energy is most effectively transferred from noise to the powerful wave ($K < 1$). The rings' size, intensity, and width can be predicted quite accurately from (11) and (13); see Fig. 5. The modulation depth in experiment is less than the theoretical estimates, which is attributed to additional noise source in the bulk of the nonlinear element.

Note that these experiments are pioneer observations of SSSF for values of B-integral order of unity, i.e., observations without

destruction of nonlinear medium. For $B \approx 1$, the intensity peak is so small that it is hardly noticeable. The authors of [17] and [18] measured the energy of the beam that had passed through a diaphragm in the focus of a lens, with the diaphragm diameter corresponding to $2 \div 3$ diffraction limits. The decrease of this energy due to SSSF occurred only for $B > 3$, when there was a high probability of nonlinear medium destruction. In our experiments, we reliably observed SSSF at $B \approx 1$, and there are ways to observe effect at $\mathrm{B} < 1$ in the future. Such measurements may be used in powerful laser systems for nondestructive diagnostics of SSSF and for measuring the B-integral.

C. Integral Spatial Noise Amplification

Power limitation associated with SSSF arises when the breakdown threshold is exceeded. Therefore, in practice, it is useful to know peak value of intensity I_{peak} and root-mean-square (rms) deviation I_{rms}. For radiation in the form of a wave having power P with noise component having power P_{n}, these quantities may be estimated by empirical formulas [16]

$$I_{\mathrm{peak}}/I_{\mathrm{aver}} = (1 + 5\sqrt{P_n/P})^2 \tag{16}$$

$$I_{\mathrm{rms}}/I_{\mathrm{aver}} = (1 + \sqrt{P_n/P})^2 - 1 \tag{17}$$

where I_{aver} is the average value of intensity. In this connection, it is interesting to know the noise amplification coefficient not for definite spatial frequencies κ, but throughout the instability interval (6) K_{int}. If the spatial spectrum width of noise at the input is much more than κ_{cr} (i.e., $\alpha_{\mathrm{dust}} \gg 2\alpha_{\mathrm{cr}}$, which frequently occurs in real conditions), then

$$K_{\mathrm{int}}(B, l, L) = \frac{P_{\mathrm{out}}}{P_{\mathrm{in}}} = \frac{2}{\kappa_{\mathrm{cr}}^2} \int_0^{\kappa_{\mathrm{cr}}} K(B, \varphi_{\mathrm{in}}(l, L, \kappa), \kappa)\kappa d\kappa \tag{18}$$

where $P_{\mathrm{in,out}}$ is the noise power in the interval (6) at the input and output of the nonlinear medium, $K(B, \varphi_{\mathrm{in}}, \kappa)$ is found from (11), and φ_{in} from (13). Strictly speaking, the amplification coefficient K may be a little more than unity outside the interval (6) as well (see Fig. 2), but we will restrict our averaging to this interval. Analysis of the function $K_{\mathrm{int}}(B = \mathrm{const}, l)$ demonstrates that it has peaks in the region of negative l and two dips: one at $l > 0$ and the other at $l < 0$ (see the insert in Fig. 6). In Fig. 6, we show the functions $K_{\mathrm{int}}(B)$ for extreme values of $l, K_{\max}(B) = \exp(2B)$, as well as the amplification $K_{\mathrm{av}}(B)$ averaged over l. The latter function corresponds to the noise source uniformly distributed along the z-axis for both $l > 0$ and $l < 0$. One can determine from Fig. 6 the value of K_{int} for the best and worst positions of noise source, as well as for the case when a noise source is distributed in space, K_{av}. From (11), (18) one can readily find

$$K_{\mathrm{av}}(B) = 1 + 2\int_0^1 \frac{\sinh^2(Bx)}{x\sqrt{1-x^2}}dx \approx \cosh(1.83B). \tag{19}$$

Fractional error of the approximate equality is well seen in Fig. 6 (cf. the dark triangles and the dotted curve). Note that K_{av} is much less than $K_{\max} = \exp(2B)$, which is the quantity that is frequently used for estimates.

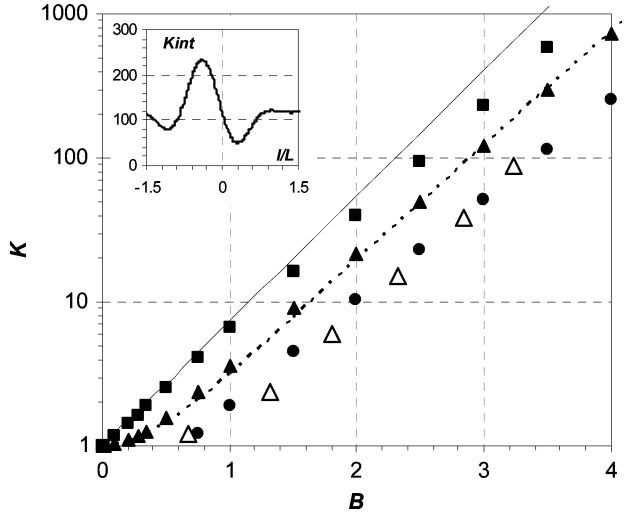

Fig. 6. Function $K_{\mathrm{int}}(B)$ for extreme values of the distance l to noise source (function $K_{\mathrm{int}}(l/L)$ for $B = 3$ is shown in the insert): maximum (squares), minimum (circles); as well as functions $K_{\mathrm{av}}(B)$ (dark triangles are for exact equality in (19), dotted line is for approximate equality) and $K_{\max}(B) = \exp(2B)$ (thin line). Open triangles designate function $K_{\mathrm{av}}(B)$ for laser amplifier with the following parameters: $L = 33$ cm, saturation energy 3.5 J/cm^2, small-signal gain 2.9, $n = 1.582, n_2 = 1.2 \cdot 10^{13}$ esu, noise source (opaque spots 100 m) is uniformly distributed along the z-axis in the interval $3L < l < 3L$.

Let us assess the values of the B-integral $B_{\max}$ at which $I_{\mathrm{peak}} = 2I_{\mathrm{aver}}$ at the output from the nonlinear medium, if the peak value of intensity at the input is 10% higher than the average value. From (16), it follows that, in this case, we have $K_{\mathrm{int}} = 72$. It is clearly seen in Fig. 6 that, for the noise sources located at most dangerous distances, $K_{\mathrm{int}} = 72$ for $B_{\max} = 2.4$, for the noise sources at most safe distances for $B_{\max} = 3.2$, and for the noise sources uniformly distributed in space, for $B_{\max} = 2.7$. If noise power is lower in the input radiation, higher values of B-integral that are readily found from (16) and Fig. 6 are admissible. In particular, it is easy to show from (16), (18), and Fig. 6 that a $\sim$6-fold decrease of noise power in the input beam allows one to increase $B_{\max}$ by unity.

D. SSSF in Two Nonlinear Media Separated by an Air Gap

Partitioning of a nonlinear medium into two parts separated by an air gap (Fig. 1) decreases SSSF in the majority of cases. This fact was investigated both in theoretical [16], [17], [19]–[21] and experimental [18], [22] works. If a Kepler telescope is available between two nonlinear media, then, by placing the diaphragm into its focal plane, one can substantially reduce noise at high spatial frequencies, thus decreasing SSSF. This is the principal way of SSSF reduction.

In some cases, such a method of SSSF suppression is ineffective or even impossible. First, for beams whose diameter is less than 3 cm, the difference between the angle $\alpha_{\max}$ for which SSSF has maximal increment and the diffraction angle is small. In this case, image relay by the Kepler telescope is accomplished without a diaphragm. Second, for considerations of laser facility compactness and simplicity, it is sometimes reasonable not to use a telescope between two amplifiers of the same diameter. In these cases, SSSF may be controlled by changing the distance between two nonlinear media, l_2. Note that, when image relay is used, l_2 may be either larger or smaller than zero.

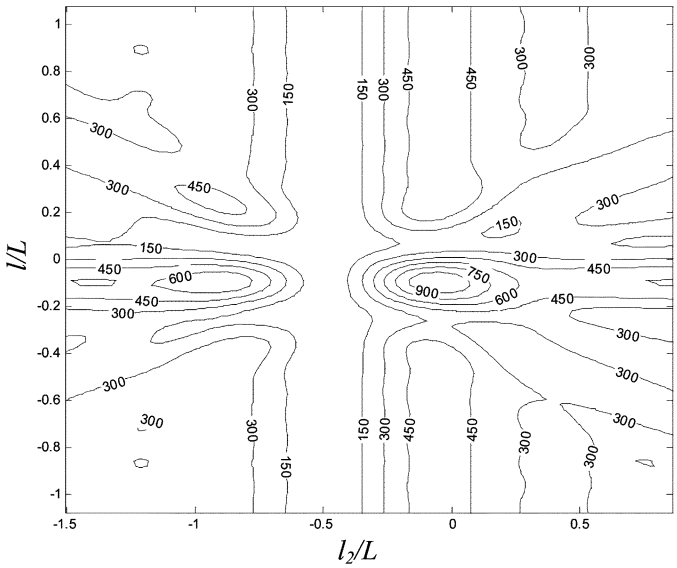

Fig. 7. Function $K_{\rm int}(l/L, l_2/L)$ for two nonlinear media of length L separated by a gap having length l_2 (l is the distance from the noise source). The total value of B-integral in two nonlinear media is $B_\Sigma = 3.8$.

Let us calculate how the amplification coefficient $K_{2\rm int}$ integral at all spatial frequencies in the band equation (6) depends on l_2. For this, we will find the transformation matrix $\mathbf{U}_2$ for two identical nonlinear media having length L

$$\mathbf{U}_2 = \mathbf{U}\mathbf{U}_{\rm air}\mathbf{U} \tag{20}$$

where the air gap transformation matrix $\mathbf{U}_{\rm air}$ is determined from (10) for $B = 0$. The substitution of (20) for (10) into (9) yields $K_{2\rm int}$ analogously to (18). Omitting bulky expressions, we just note that $K_{2\rm int}$ depends only on $l/L, l_2/L$ and the B-integral. In Fig. 7 $K_{2\rm int}(l/L, l_2/L)$ is shown for $B = 1.9$, i.e., the total the B-integral is $B_\Sigma = 3.8$.

As is seen in Fig. 7, the function $K_{2\rm int}(l/L)$ has two well-pronounced maxima and one minimum at $l < 0$. In Fig. 8, we show $K_{2\rm int}(l_2/L)$ for extreme values of l, as well as an average value of $K_{2\rm av}(l_2/L)$ for noise sources uniformly distributed in the interval $1.5L > l > 1.5L$ outside which the value of $K_{2\rm int}(l)$ changes only slightly (see Fig. 7). As is clear from Fig. 9, for any l, $K_{2\rm int}$ is maximal at $l_2 \approx 0$ and minimal at $l_2 = l_{2\min} < 0$. This agrees qualitatively with conclusions of the earlier studies on SSSF suppression [16]–[21]. Physically, the minimum of $K_{2\rm int}$ and $K_{2\rm av}$ for $l_2 = l_{2\min}$ is explained by the fact that the perturbation phase at the output of the first nonlinear medium, $\varphi_{\rm out}$, weakly depends on l (i.e., on noise source position); see Fig. 3. It is seen in this figure that, for angles α close to $\alpha_{\max}$, $\varphi_{\rm out1} \approx -\pi/4$. According to (13), the perturbation phase at the input to the second nonlinear medium will be

$$\varphi_{\rm in2}(\alpha = \alpha_{\max}) \approx -\frac{\pi}{4} + \frac{\alpha^2}{2} k n_0 l_2. \tag{21}$$

It is apparent from Fig. 2 that the necessary condition for minimization of the amplification coefficient is $\varphi_{\rm in2}(\alpha = \alpha_{\max}) = -3\pi/4$. The same condition also follows from (15). Then, taking into account (21), we obtain

$$l_{2\min} = -\frac{\pi L}{n_0 B_\Sigma}. \tag{22}$$

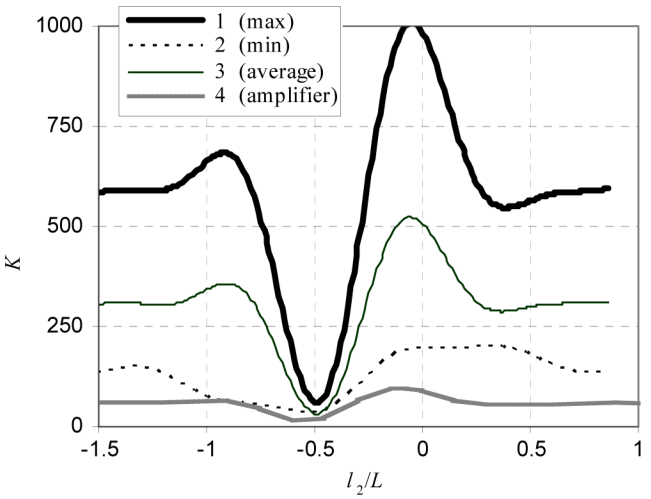

Fig. 8. Functions $K_{2\rm int}(l_2/L, B_\Sigma = 3.8)$ for two passive nonlinear media plotted for most (1) and least (2) dangerous distance to noise source ($l/L = 0.11$ and $l/L = 0.078$) and function $K_{2\rm av}(l_2/L)$ (3) for the noise sources (opaque spots 100 m) uniformly distributed on the interval $1.5 > l/L > 1.5$. Curve (4) shows function $K_{2\rm av}(l_2/L)$ for two laser amplifiers having the following parameters: pulse duration 1 ns, $\lambda = 1055$ nm, energy density at the input 1.39 J/cm^2, saturation energy 3.5 J/cm^2, small-signal gain in each amplifier 2.9, $L = 33$ cm, $n_0 = 1.58, n_2 = 1.2 \cdot 10^{-13}$ esu, and $B_\Sigma = 3.8$.

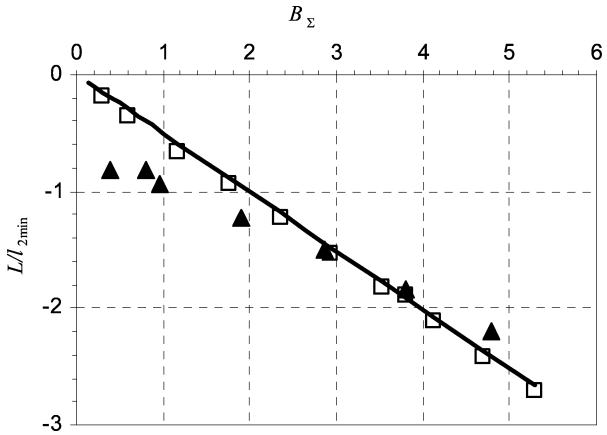

Fig. 9. Functions $l_{2\min}(B_\Sigma)$ for passive nonlinear media: numerical squares and analytical equation (22) straight line. Triangles show analogous dependence for two laser amplifiers with parameters as in Fig. 8.

From this formula, one can readily find an optimal distance between the nonlinear media. From Fig. 9, where the function $l_{2\min}(B_\Sigma)$ is plotted it is clear that formula (22) is very accurate. Note that, in spite of numerous works [16]–[21] concerned with SSSF suppression at negative $l_{2\min}$, we were the first to obtain (22). The authors of [17] showed that, if $B_\Sigma = \pi$, then $l_{2\min} = -L/n_0$, which is a particular case of (22). A semi-empirical formula was derived in [16] for $l_{2\min}(B_\Sigma)$ in the case of noise filtering in a relay by a diaphragm with angular size of order $\alpha_{\max}$, but, for $\alpha = \alpha_{\rm cr}$, it gives a 25%–30% error. At the same time, (22) gives a correct value for arbitrary $\alpha < \alpha_{\rm cr}$.

The function $K_{2\rm av}(B_\Sigma)$ is plotted in Fig. 10 for extreme values of l_2: maximum at $l_2 \approx 0$ [well described by (19)] and minimum at $l_2 = l_{2\min}$. It is clear from this figure that the minimal value of $K_{2\rm av}(B_\Sigma, l_2 = l_{2\min})$ is described well by the formula

$$K_{2\rm av}(B_\Sigma, l_2 = l_{2\min}) = \cosh^2(0.65 B_\Sigma). \tag{23}$$

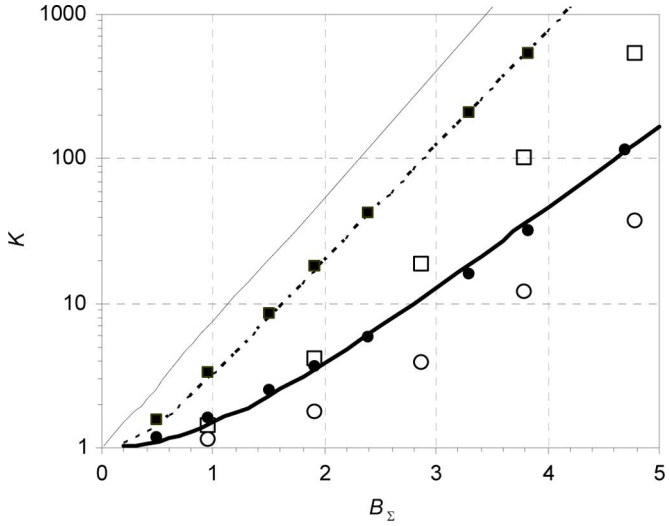

Fig. 10. Functions $K_{2\mathrm{av}}(B_\Sigma)$ for two passive nonlinear media separated by an air gap of most dangerous length [dark squares, dotted line—approximate equality (19)] and least dangerous length $l_{2\,\min}$ [dark circles, heavy line—(23)]. Analogous functions $K_{2\mathrm{av}}(B_\Sigma)$ for two laser amplifiers (parameters like in Fig. 8) separated by an air gap of most dangerous length (open squares) and least dangerous length (open circles). The thin line shows function $K_{2\,\max}(B_\Sigma) = \exp(2\,B_\Sigma)$.

Thus, when the condition (22) is fulfilled, $K_{2\mathrm{av}} = 72$ for $B_\Sigma = 4.3$. With allowance for (16), from this, it follows that, if the peak value of intensity at the input to a nonlinear medium is 10% higher than the average value, then $I_{\mathrm{peak}} = 2I_{\mathrm{aver}}$ at the output for $B_\Sigma = B_{\max} = 4.3$, whereas for a nonlinear medium without an air gap $(l_2 = 0)$, $B_{\max} = 2.7$ (see Section III-C).

Some reduction of $K_{2\mathrm{int}}$ and $K_{2\mathrm{av}}$ may be achieved for $l_2 > 0$ too, i.e., without image relay, which is quite useful if it is not impossible to relay images. Note that in this case one need not know the exact value of $l_{2\,\min}$ because functions $K_{2\mathrm{int}}(l_2)$ and $K_{2\mathrm{av}}(l_2)$ have no sharp minima, as in the case of $l_2 < 0$ (see Fig. 8). However, for $l_2 > 0$, reduction of $K_{2\mathrm{av}}$ and the corresponding growth of $B_{\max}$ are insignificant: $B_{\max} = 3.0$.

E. SSSF Features in Laser Amplifiers

As was noted above, the substitution of an active medium (laser amplifier) for passive changes nothing for LSSF. The situation is different for SSSF. Small-scale instability (spatial scale, phase, and amplification) depends on intensity that is increasing during propagation in the amplifier. An analytical expression for the transformation matrix $\mathbf{U}$ of the amplifying medium for the case when beam energy is much less than saturation energy of the laser transition (which is seldom realized in practice) was obtained in [5]. Thus, all of the above expressions may serve only as estimates for laser amplifiers. A more accurate prognosis may be made by means of numerical simulation of SSSF.

Numerical simulation was done using the FRESNEL software [16] with 2048×2048 grid. For SSSF in passive (nonamplifying) media, all changes of the field are local in time. Laser amplification coefficient in an active laser medium depends on pulse energy. Therefore, in numerical simulation of SSSF, it is necessary to consider the dependence of intensity on time. In all our calculations, we divided the bell-shaped 1-ns pulse into 16 time intervals.

When simulating SSSF, the noise source must be specified either at a definite distance l from the nonlinear medium or distributed along the z-axis. In the first case, we model noise sources on the surface of elements, and in the second case distributed in the bulk. We believe that, if measures against air dust are observed in laser labs and high-quality optical elements with pure surfaces are used, then laser amplifiers are the main sources of spatial noise because of their large length and plenty of microinclusions. For modeling bulk sources of noise, we placed on the beam path a large amount (up to 100) of screens with chaotically scattered nontransparent "dust particles" 100 μm in diameter. The "dust particles" were randomly distributed over the screens. The screens position was also random in the range $-3L < l < 3L$.

The amplification coefficient of perturbations K for SSSF was calculated at the time moment corresponding to the maximal B-integral [15]. In addition, we normalized the value of K to the amplification coefficient of the laser amplifier at the same moment of time so as to conserve the physical meaning of K: the amplification coefficient of perturbations relative to the powerful wave.

The function $K_{\mathrm{av}}(B)$ for the laser amplifier is shown in Fig. 6 by open triangles. As was to be expected, this dependence lies below $K_{\mathrm{av}}(B)$ for a passive medium. This is explained by the fact that the intensity grows along z, hence, maximally amplified spatial frequency is constantly changing. Thus, the considerations presented in Section III-B on maximal value of the B-integral are still valid but, other things being equal, higher values of the B-integral are admissible in an active medium.

In Section III-D, we showed that, by changing the distance l_2 between two successively located nonlinear media, one can suppress SSSF substantially. The dependence of $K_{2\mathrm{av}}$ on the distance l_2 between two amplifiers is plotted in Fig. 8 for noise sources uniformly distributed in space ahead of the first amplifier in the region $-3L < l < 3L$. If the amplifiers are arranged next to each other $(l_2 = 0)$, then $K_{2\mathrm{av}}$ will be close to a maximum value. For $l_2 = l_{2\,\min}$, a minimum value is attained which for the given parameter are ten times less than the maximum. Numerical computations demonstrate that the magnitude of $l_{2\,\min}$ is independent of the distance to the noise source l, which is similar to the case of a passive medium. It is clear from Fig. 9 that, for $2 < B_\Sigma < 4$, (22) may be used for estimation of $l_{2\,\min}$. When there is no image relay, i.e., for $l_2 > 0$, the minimum value of $K_{2\mathrm{av}}$ is two times lower than the maximum one.

In Fig. 10, the function $K_{2\mathrm{av}}(B_2)$ is plotted for two amplifiers placed at the most dangerous distance and at the most safe distance $l_{2\,\min}$. One can see that, with appropriate choice of the distance between the amplifiers, the effect of SSSF suppression occurs like in the case of passive nonlinear media. For example, with a correct choice of the distance between the amplifiers, $K_{2\mathrm{av}} = 72$ for $B_\Sigma = 5$. Taking into consideration (16), from this it follows that, if the peak intensity at the input to the nonlinear medium is 10% higher than the average value, then at the output we will have $I_{\mathrm{peak}} = 2I_{\mathrm{aver}}$ for $B_\Sigma = B_{\max} = 5$.

In spite of the fact that $K_{2\mathrm{av}}(l_2)$ [Fig. 8, curve (4)] is universal for any random noise, intensity distribution depends on concrete noise. RMS deviations of intensity I_{rms} and maximal value of intensity I_{peak}, as well as curves plotted by (16) and (17) with allowance for $K_{2\mathrm{av}}(l_2)$ (see Fig. 8) are presented in Fig. 11. It

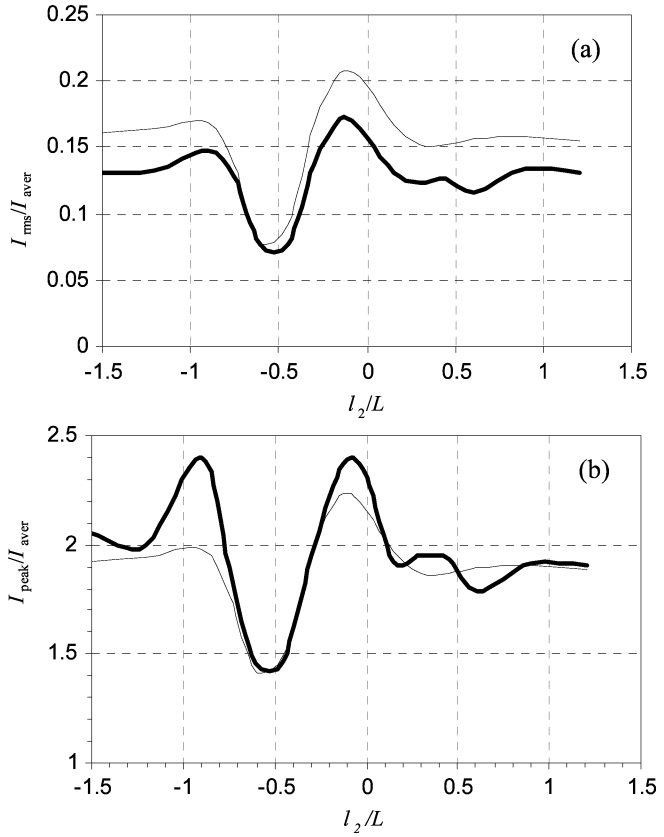

Fig. 11. RMS deviation of (a) intensity $I_{\rm rms}$ and (b) peak intensity $I_{\rm peak}$ as a function of l_2/L for two laser amplifiers with parameters like in Fig. 8. Heavy lines are for numerical calculations, and thin lines are for (16) and (17) with allowance for $K_{2\rm av}(l_2/L)$ plotted in Fig. 8.

is clear from Fig. 11(a) that the dependences $I_{\rm rms}(l_2)$ obtained by (17) and numerically coincide topologically, but (17) gives slightly overestimated values. This is evidently explained by the nonuniformity of the spatial spectrum of noise due to nonlinearity of amplification of different noise frequencies, as well as by the nonlinear character of laser amplification.

In terms of breakdown, $I_{\rm peak}$ is the most significant characteristic of a laser beam. Our calculations [Fig. 11(b)] demonstrate that, upon the whole, the values of $I_{\rm peak}$ correlate sufficiently well with the values obtained by (16). At the same time, a pronounced peak appears for $l_2/L = -0.9$, although the increase in $K_{2\rm av}(l_2)$ and $I_{\rm rms}(l_2)$ is insignificant [Figs. 8, 11(a)]. The value of this peak is different for different noise [not shown in Fig. 11(b)], but it is always higher than those given by (17). As a result, there are "hot speckles" at rather smooth intensity distribution. These "hot speckles" are explained by simultaneous action of cubic nonlinearity and laser gain saturation nonlinearity. Hence, they have another nature than the "hot images" observed in [23], [24] which are explained by image relay by cubic nonlinear medium. Taking into account that these "hot speckles" arise at the values of l_2 close to $l_{2\,\rm min}$, one should avoid them when creating powerful laser amplifiers.

IV. Conclusion.

The analysis of possible causes of power limitation of nanosecond Nd:glass lasers showed that SSSF is the main one of them.

We were the first to observe in experiment amplification of laser beam noise component for the B-integral (nonlinear phase) less than unity, i.e., when a nonlinear medium is not destructed. The results agree well with the theoretical predictions. Such measurements may be used in powerful laser systems for nondestructive diagnostics of SSSF and for measuring the B-integral.

The dependence equation (19) of the noise amplification coefficient on B-integral in one layer of a passive (without laser amplification) nonlinear medium was found. If the ratio of peak intensity to averaged intensity at the input to the medium is 1.1 and at the output this ratio must be less than 2, then the maximum allowable value of the B-integral will be $B_{\rm max} = 2.7$. A sixfold reduction of noise power in the input beam allows one to increase $B_{\rm max}$ by unity.

For two nonlinear media separated by an air gap with image relay, SSSF may be suppressed substantially, especially if an image is relayed from the output plane of the first medium at an optimal distance inside the second nonlinear medium. We have obtained a simple dependence equation (22) of this distance on the B-integral, as well as the dependence equation (23) of the noise amplification coefficient on B-integral. The allowable value of the B-integral in this case increases up to $B_{\rm max} = 4.3$. If it is impossible to use a relay, then one can suppress SSSF by choosing distances between nonlinear media, but allowable values B-integral will be less in this case: $B_{\rm max} = 3.0$.

Upon the whole, the results obtained for amplifying nonlinear media are analogous to those for passive media, but the values of $B_{\rm max}$ are about 0.5 higher. At the same time, the results of numerical computation demonstrate that for $B < B_{\rm max}$ some hot speckles may appear in amplifying nonlinear media that lead to breakdown.

In neodymium-phosphate glass lasers with rod amplifiers 10 cm in diameter, the maximum admissible energy is 400 J with pulse duration of 1 ns. A detailed description of 300-J/1-ns Nd:glass laser setup will be given in Part II of this study [25].

References

[1] V. V. Lozhkarev, G. I. Freidman, V. N. Ginzburg, E. V. Katin, E. A. Khazanov, A. V. Kirsanov, G. A. Luchinin, A. N. Mal'shakov, M. A. Martyanov, O. V. Palashov, A. K. Poteomkin, A. M. Sergeev, A. A. Shaykin, and I. V. Yakovlev, "Compact 0.56 petawatt laser system based on optical parametric chirped pulse amplification in KD*P crystals," *Laser Phys. Lett.*, vol. 4, pp. 421–427, 2007.

[2] J. Bunkenberg, J. Boles, D. C. Brown, J. Eastman, J. Hoose, R. Hopkins, L. Iwan, S. D. Jacobs, J. H. Kelly, S. Kumpan, S. Letzring, D. Lonobile, L. D. Lund, G. Mourou, S. Refermat, W. Seka, J. M. Soures, and W. Ken, "The omega high-power phosphate-glass system: Design and performance," *IEEE J. Quantum Electron.*, vol. QE-17, no. 9, pp. 1620–1628, Sep. 1981, 1981.

[3] V. I. Bayanov, E. G. Bordachev, V. I. Kryzhanovskiĭ, V. A. Serebryakov, O. S. Shchavelev, A. V. Charukhchev, and V. E. Yashin, "High-gain phosphate neodymium glass rod amplifiers with 60 mm diameter," *Sov. J. Quantum Electron.*, vol. 14, pp. 213–216, 1984.

[4] V. I. Bespalov and V. I. Talanov, "Filamentary structure of light beams in nonlinear liquids," *JETP Lett.*, vol. 3, pp. 307–310, 1966.

[5] N. N. Rozanov and V. A. Smirnov, "Small-Scale self-focusing of the laser radiation in amplifying systems," *Sov. J. Quantum Electron.*, vol. 10, pp. 232–240, 1980.

[6] W. H. Lowdermilk and D. Milam, "Laser-induced surface and coating damage," *IEEE Journal of Quantum Electronics*, vol. QE-17, no. 12, pp. 1888–1902, Dec. 1981.

[7] W. Koechner, *Solid-State Laser Engineering*. Berlin, Germany: Springer, 1999.

[8] N. G. Bondarenko, I. V. Evemina, and A. I. Makarov, "Measurement of the coefficient of electronic nonlinearity in optical and laser glass," *Sov. J. Quantum Electron.*, vol. 8, pp. 482–484, 1978.
[9] V. N. Gol'dberg, V. I. Talanov, and R. E. Erm, "," *Izv. VUZov. Radiofizika*, vol. 10, pp. 674–685, 1967.
[10] *Lasers and Laser-Related Equipment—Test Methods for Laser Beam Widths, Divergence Angles and Beam Propagation Ratios—Part 2: General Astigtic Beams*, Standard ISO 11146-2:2005, 2005.
[11] S. N. Vlasov, V. A. Petrishchev, and V. I. Talanov, "Averaged description of wave beams in linear and nonlinear media," *Izv. VUZov. Radiophysics*, vol. 14, pp. 1353–1363, 1971.
[12] A. K. Poteomkin and E. A. Khazanov, "Calculation of the laser-beam M2 factor by the method of moments," *Quantum Electron.*, vol. 35, pp. 1042–1044, 2005.
[13] E. Perevezentsev, A. Poteomkin, and E. A. Khazanov, "Comparison for phase aberrated laser beams quality criteria," *Appl. Opt.*, vol. 46, pp. 774–784, 2007.
[14] A. I. Makarov and A. K. Poteomkin, "On brightness transformation when multiplying frequency of multimode radiation," *Izv. VUZov. Radiophysics*, vol. 30, pp. 1484–, 1987.
[15] M. A. Martyanov, G. A. Luchinin, A. K. Poteomkin, and E. A. Khazanov, "Linear dependence of the time shift of an amplified pulse on the energy extraction from a laser amplifier," *Quantum Electron.*, vol. 38, pp. 103–108, 2008.
[16] S. G. Garanin, I. V. Epatko, L. V. L'vov, R. V. Serov, and S. A. Sukharev, "Self-focusing suppression in a system of two nonlinear media and a spatial filter," *Quantum Electron.*, vol. 37, pp. 1159–1165, 2007.
[17] S. N. Vlasov and V. E. Yashin, "Self-focusing suppression in neodymium glass laser systems by means of relays," *Sov. J. Quantum Electron.*, vol. 11, pp. 313–321, 1981.
[18] N. B. Baranova, N. E. Bykovskii, Y. V. Senatskii, and S. V. Chekalin, "Nonlinear processes in an optical medium of powerful neodymium lasers," *Proc. P.N. Lebedev Phys. Inst. USSR Acad. Sci.*, vol. 103, pp. 84–117, 1978.
[19] S. N. Vlasov, "Instability of a high-intensity plane wave in a periodic nonlinear medium," *Sov. J. Quantum Electron.*, vol. 6, pp. 245–246, 1976.
[20] S. N. Vlasov, "Stabilization of plane-wave instability in a periodic system," *JETP Lett.*, vol. 4, pp. 795–800, 1978.
[21] S. M. Babichenko, N. E. Bykovskii, and Y. V. Senatskii, "Possible reduction of nonlinear losses at small-scale self-focusing in a piecewise-continuous medium," *Sov. J. Quantum Electron.*, vol. 12, pp. 105–106, 1982.
[22] N. B. Baranova, N. E. Bykovskii, B. Zel'dovich, and Y. V. Senatskii, "Diffraction and self-focusing of radiation in a powerful optical pulse amplifier," *Sov. J. Quantum Electron.*, vol. 4, pp. 1354–1361, 1974.
[23] W. H. Williams, K. R. Manes, J. T. Hunt, P. A. Renard, D. Milam, and D. Eimerl, "Modeling of self-focusing experiments by beam propagation codes," *ICF Quarterly Rep.*, vol. 6, pp. 7–14, 1995.
[24] J. T. Hunt, K. R. Manes, and P. A. Renard, "Hot images from obscurations," *Appl. Opt.*, vol. 32, pp. 5973–5982, Oct. 20, 1993, 1993.
[25] A. K. Poteomkin, A. V. Kirsanov, M. A. Martyanov, E. A. Khazanov, and A. A. Shaykin, "Compact 300 J/300 GW frequency doubled neodimium glass laser—Part II: Laser setup," *IEEE J. Quantum Electron.*, to be published.

Anatoly K. Potemkin was born in Nizhny Novgorod (former Gorky), Russia, in 1949. He received the M.S. degree in physics from the Nizhny Novgorod State University, Nizhny Novgorod, in 1973.

Since that time, he has been with the Institute of Applied Physics, Russian Academy of Science, Nizhny Novgorod. He is the author of more than 200 papers concerning laser optics, nonlinear optics, and spectroscopy.

Efim A. Khazanov was born in Nizhny Novgorod (formerly Gorky), Russia, in 1965. He received the Ph.D. and Doctor of science degrees in physics and mathematics from the Institute of Applied Physics, Russian Academy of Science, Nizhny Novgorod, in 1992 and 2005, respectively.

In 2008, he was elected as a Corresponding Member of the Russian Academy of Science. His research is in the field of phase conjugation of depolarized radiation, stable narrow-bandwidth Q-switch lasers, diffraction-limited solid-state lasers with both high pick and average power, thermooptics of solid-state lasers including ceramics lasers, optical parametrical amplification of chirped pulse, and petawatt lasers. He is the author or coauthor of more than 70 papers. He is currently the head of the department of the Institute of Applied Physics, Russian Academy of Sciences, and Professor with Nizhny Novgorod State University.

Mikhail A. Martyanov was born in Nizhny Novgorod, Russia, in 1979. He received the M.S. degree in physics from the Nizhny Novgorod State University, Nizhny Novgorod, in 2002. He is currently working toward the Ph.D. degree at the Institute of Applied Physics, Russian Academy of Science, Nizhny Novgorod.

His current research interests are solid-state lasers and nonlinear optics.

Mar'yana S. Kochetkova was born in Nizhny Novgorod, Russia, in 1986. She received the B.S. degree in physics from the Nizhny Novgorod State University, Nizhny Novgorod, in 2008. She is currently working toward the M.S. degree at the Institute of Applied Physics, Russian Academy of Science, Nizhny Novgorod.

Her current research interests are solid-state lasers and nonlinear optics.